Angular Velocity Estimation Using Rate-Integrating Gyro Measurements

S.P. Arjun Ram*, Maruthi R. Akella†, and Renato Zanetti ‡
Department of Aerospace Engineering and Engineering Mechanics, The University of Texas at Austin, Austin, Texas 78712

Rate Integrating Gyroscopes (RIGs) measure integrated angular rates or angular displacement, requiring an observer to provide full state feedback to the attitude controller. The problem of estimating the angular velocity of a rotating rigid body with known torque, using measurements from a rate integrating gyro is considered. A nonlinear observer is designed for cases when the inertia is accurately known as well as an adaptive observer for unknown inertia, that uses only continuous-time RIG measurements and provides estimates of the angular velocity. Moreover, the non-adaptive observer is shown to be robust to bounded inaccuracies in the knowledge of inertia and external torque acting upon the system while the state estimation error converges exponentially to zero when the model is perfect and asymptotically when adapting for inaccurate inertia. The adaptive observer proposes a novel update rule for parameter adaptation involving additional control knobs using the attitude states to overcome the unavailability of the angular rate states as required by conventional certainty equivalence methods. The observer is tested in simulation to demonstrate its effectiveness.

*Graduate Research Assistant, Email: arjun.ram@utexas.edu
†Ashley H. Priddy Centennial Professor, Email: makella@mail.utexas.edu. AIAA Fellow
‡Assistant Professor, Email: renato@mail.utexas.edu. AIAA Associate Fellow

I. Introduction

Inertial navigation is a critical component of aerospace control systems for the calculation of position, velocity and orientation using measurements from Inertial Measurement Units (IMUs). These systems are usually comprised of accelerometers and gyroscopes and integrate forward in time the initial state of the vehicle by replacing dynamic models with IMU measurements. Inertial navigation systems have been used since the 1950s and were popularly part of the Apollo missions on the Saturn V rockets, the command module and the lunar module. In a strapdown inertial navigation system [1], the IMU is rigidly mounted on the vehicle. Strapdown gyroscopes have been used for many applications including spacecraft attitude estimation [2], underwater vehicle navigation [3], human navigation systems [4] and robotic navigation [5].

One approach to attitude determination is to integrate Euler's equation using models of the torques applied to the vehicle. Alternatively, inertial navigation bypasses the need for these models by measuring angular velocity directly (referred to as model replacement mode [6]). This methodology is preferred when IMU information is more accurate than the available models of rotational dynamics and torques. Moreover, model replacement is computationally much simpler for real-time onboard applications.

Rate Integrating Gyroscopes (RIGs) do not directly measure the angular rate but rather accumulate angular displacements by integrating the feedback required to null internal gyroscope motions. They provide measurements of the integrated rate and thus provide a direct measurement of neither the attitude state nor the angular velocity. They are preferred in spacecraft applications compared to conventional rate gyroscopes for their low noise due to degenerate mode operation and exceptional scale factor stability [7]. Modern RIGs use micro-electromechanical system devices [8].

Attitude controllers for aerospace systems typically require state feedback, where the state consists of the attitude and angular rate. However, since rate integrating gyroscopes do not provide angular rate measurements, state feedback controllers would require an observer to reconstruct the full state using the IMU measurements. Kalman filters have been used in the literature to estimate this state [9,10]. For gyroscopes systems that measure angular velocity directly, nonlinear observers for

attitude and gyro bias with exponential stability exist [11,12]. This work, on the other hand, focuses on designing observers for known and adaptive inertia cases, which use continuous measurements from an RIG and provides estimates for the angular rate states that converge (exponentially when the inertia is known) to their true values when the external torques are perfectly modeled. The angular velocity estimates provided by these observers can be used in controllers for stabilizing the system or tracking desired reference trajectories. To the best of our knowledge, no prior work exists in the literature on continuous time observers for RIG systems.

RIGs are used for high precision applications because they provide the entire history of the angular velocity as its integrated value. The alternative of sampling the angular velocity at discrete times is typically less accurate as information on how the angular velocity varies in-between samples is lost. While we use continuous time RIG measurements here, discretizing the output of a continuous observer such as the one presented in this work will help use this observer with discrete time computer systems, while preserving the theoretical guarantees presented for the observer and the inherent advantages of using RIGs.

In this work, we consider a rigid body governed by Euler rotational dynamics, the angular rotational rate is assumed to satisfy a known upper bound and the torque applied is known. We present two nonlinear observer designs, for the known inertia and adaptive cases, which utilize the measurements from the RIG and provide estimates of the angular rate states. The observer dynamics are linear in the measurement term and involve a user chosen parameter that controls the convergence rate.

When IMUs are used in space applications, in the context of on-orbit assembly, repair and refilling missions, perfect knowledge of the inertia matrix is often not always available and therefore necessitates the use of adaptive observers that can deal with model parameter uncertainties. We present an adaptive nonlinear observer design, which provides estimates of the angular rate states while adapting for the inertia terms. Unlike the certainty equivalence adaptive methods, the design of this observer, inspired by the Immersion and Invariance (I & I) control method [13], includes two extra adaptation parameters which helps compensate for the dynamics of the unmeasured terms. In

the adaptive case, the rate of change of the torque applied is also assumed to be known.

A Lyapunov-like analysis is used to prove that the attitude and angular velocity state estimates converge to the true values as long as the initial states are within a Region Of Attraction (ROA), hence the result is semi-global. With adaptation, the inertia terms can be estimated to the true value asymptotically if persistence of excitation conditions are met. Further, the non-adaptive observer is shown to have exponential convergence, be robust to inaccuracies in the inertia matrix and the external torque and the estimates converge to the true states within a residual set as long as the errors in inertia and torque are bounded. These results are demonstrated in numerical simulations.

Extending the observer to adapt for inertia uncertainties using conventional adaptive observer methods is not straightforward since the available measurements from the RIG are only of the angular displacement while the inertia matrix is only part of the dynamics involving the angular velocity. Methods inspired by Cho and Rajamani [14] require the measurement outputs to have a strictly positive definite transfer function to the unknown inertia parameters, which is not the case in this system as will be discussed in the sequel. Moreover, the measurement here is the integrated angular rate vector and hence Marino and Tomei's [15] method of linearizing the system on the basis of output injection and filtered transformations cannot be used, since it requires the output to be a real valued scalar or linear with respect to the unknown parameters. Observers for multi-output systems which are affine in the unmeasured states [16] can also not be used since the dynamics are not linear in the angular velocity states.

The paper is organized as follows: the dynamics are introduced and the estimation problem is stated in the next section. The observer formulation and the Lyapunov-like analysis for known inertia is presented for its convergence properties. The next section presents an observer design for the adaptive inertia case with a similar Lyapunov-like convergence analysis. The robustness of the non-adaptive observer to inertia and torque inaccuracies is discussed in the following section. The simulation section follows, which performs numerical analysis of the observer system for the different scenarios before wrapping up with the conclusions in the final section. Throughout this paper, uppercase letters are used to denote matrices and bold faced variables denote vectors. For

any symmetric matrix P, the notation $\lambda_{\min}(P)$ and $\lambda_{\max}(P)$ respectively denote the minimum and maximum eigenvalues.

II. Known Inertia

A. Dynamics

Consider Euler rotational dynamics for a system with inertia matrix $J = J^T > 0$ subject to bounded external torque $\boldsymbol{\tau}$ given by

$$J\dot{\boldsymbol{\omega}} = -\boldsymbol{\omega}^* J\boldsymbol{\omega} + \boldsymbol{\tau} \tag{1}$$

wherein $\boldsymbol{\omega}(t) \in \mathbb{R}^3$ has components in the body-fixed frame of reference. The skew-symmetric matrix $\boldsymbol{\omega}^*$ represents the vector cross product. We also assume:

- J is perfectly known
- $\boldsymbol{\tau}$ is perfectly determined
- $\boldsymbol{\omega} \in \mathbb{L}\infty$ is a bounded signal and we know $\omega_m \triangleq \sup_{t\geq 0} \|\boldsymbol{\omega}(t)\|$

The assumption that an upper bound ω_m is known is reasonable since any spacecraft is physically designed to only be able to rotate or tumble below a certain angular rate. The bound can be chosen beyond the design limits of the spacecraft.

B. Measurements

We have an RIG providing attitude measurements $\boldsymbol{\sigma}(t) \in \mathbb{R}^3$ which are the integrated values of the angular rate $\boldsymbol{\omega}$:

$$\dot{\boldsymbol{\sigma}} = \boldsymbol{\omega} \tag{2}$$

where $\boldsymbol{\sigma}(t)$ is assumed to be measured perfectly.

C. Objective

Using perfect measurements of $\boldsymbol{\sigma}(t)$, the goal is to generate an estimate $\hat{\boldsymbol{\omega}}(t)$ of the true angular rate $\boldsymbol{\omega}(t)$ such that

$$\lim_{t\to\infty} \|\hat{\boldsymbol{\omega}}(t) - \boldsymbol{\omega}(t)\| = 0 \tag{3}$$

keeping all signals bounded.

D. Observer Design

The following observer design is proposed for estimating the angular rate:

$$\dot{\hat{\boldsymbol{\sigma}}} = \hat{\boldsymbol{\omega}} - k(\hat{\boldsymbol{\sigma}} - \boldsymbol{\sigma}) \quad \text{for some } k > 0 \tag{4}$$

$$J\dot{\hat{\boldsymbol{\omega}}} = -\hat{\boldsymbol{\omega}}^* J\hat{\boldsymbol{\omega}} + \boldsymbol{\tau} - k^2 J(\hat{\boldsymbol{\sigma}} - \boldsymbol{\sigma}) \tag{5}$$

We define the estimation errors

$$\boldsymbol{\sigma}_e = \hat{\boldsymbol{\sigma}} - \boldsymbol{\sigma} \tag{6}$$

$$\boldsymbol{\omega}_e = \hat{\boldsymbol{\omega}} - \boldsymbol{\omega} \tag{7}$$

Using these definitions in (4)-(5) gives

$$\dot{\boldsymbol{\sigma}}_e = \boldsymbol{\omega}_e - k\boldsymbol{\sigma}_e \tag{8}$$

$$J\dot{\boldsymbol{\omega}}_e = (\hat{\boldsymbol{\omega}}^* J\hat{\boldsymbol{\omega}} - \boldsymbol{\omega}^* J\boldsymbol{\omega}) - k^2 J\boldsymbol{\sigma}_e \tag{9}$$

Expanding the terms within the parenthesis on the right-hand side of (9) gives

$$\hat{\boldsymbol{\omega}}^* J\hat{\boldsymbol{\omega}} - \boldsymbol{\omega}^* J\boldsymbol{\omega} = \boldsymbol{\omega}_e^* J\boldsymbol{\omega} + \boldsymbol{\omega}^* J\boldsymbol{\omega}_e + \boldsymbol{\omega}_e^* J\boldsymbol{\omega}_e \tag{10}$$

If we define $\boldsymbol{\Psi} \triangleq \left[\boldsymbol{\omega}^* J\boldsymbol{\omega}_e + \boldsymbol{\omega}_e^* J\boldsymbol{\omega} + \boldsymbol{\omega}_e^* J\boldsymbol{\omega}_e\right]$, Eq. 9 can be rewritten as

$$\dot{\boldsymbol{\omega}}_e = -k^2\boldsymbol{\sigma}_e + J^{-1}\boldsymbol{\Psi} \tag{11}$$

If we define the error states to be $\boldsymbol{\sigma}_e$ and $\boldsymbol{\omega}_e/k$, using (4) and (11), we have the dynamics for the error states as:

$$\begin{bmatrix} \dot{\boldsymbol{\sigma}}_e \\ \frac{\dot{\boldsymbol{\omega}}_e}{k} \end{bmatrix} = k \begin{bmatrix} -\mathbb{I}_{3\times3} & \mathbb{I}_{3\times3} \\ -\mathbb{I}_{3\times3} & \mathbb{O}_{3\times3} \end{bmatrix} \begin{bmatrix} \boldsymbol{\sigma}_e \\ \frac{\boldsymbol{\omega}_e}{k} \end{bmatrix} + \begin{bmatrix} \mathbb{O}_{3\times1} \\ \frac{J^{-1}}{k}\boldsymbol{\Psi} \end{bmatrix} \tag{12}$$

Renaming the states as

$$\begin{aligned} z_1 &= \boldsymbol{\sigma}_e \\ z_2 &= \tfrac{\boldsymbol{\omega}_e}{k} \end{aligned} \quad \Leftrightarrow \quad z \triangleq \begin{bmatrix} z_1 \\ z_2 \end{bmatrix} \in \mathbb{R}^6 \tag{13}$$

allows us to express (12) as

$$\dot{z} = k \begin{bmatrix} -\mathbb{I}_{3\times3} & \mathbb{I}_{3\times3} \\ -\mathbb{I}_{3\times3} & \mathbb{O}_{3\times3} \end{bmatrix} z + \begin{bmatrix} \mathbb{O}_{3\times1} \\ \frac{J^{-1}}{k}\boldsymbol{\Psi} \end{bmatrix} \tag{14}$$

Since the inertia matrix is known, we can use its maximum and minimum eigenvalues to express

$$J_M = \lambda_{\max}(J) = \|J\| \tag{15}$$

$$J_m = \lambda_{\min}(J) = \frac{1}{\|J^{-1}\|} \tag{16}$$

Define

$$\alpha \triangleq (J_M/J_m) \tag{17}$$

Revisiting the $\boldsymbol{\Psi}$ term introduced after Eq. 10, we have

$$\boldsymbol{\Psi} = \boldsymbol{\omega}^* J\boldsymbol{\omega}_e + \boldsymbol{\omega}_e^* J\boldsymbol{\omega} + \boldsymbol{\omega}_e^* J\boldsymbol{\omega}_e \tag{18}$$

$$\frac{J^{-1}}{k}\boldsymbol{\Psi} = \frac{J^{-1}}{k}\left(\boldsymbol{\omega}^* J\boldsymbol{\omega}_e + \boldsymbol{\omega}_e^* J\boldsymbol{\omega}\right) + \frac{J^{-1}}{k}\boldsymbol{\omega}_e^* J\boldsymbol{\omega}_e \tag{19}$$

Consider the norm of the first term

$$\|\frac{J^{-1}}{k}\left(\boldsymbol{\omega}^* J\boldsymbol{\omega}_e + \boldsymbol{\omega}_e^* J\boldsymbol{\omega}\right)\| \leq \frac{2J_M}{kJ_m}\omega_m\|\boldsymbol{\omega}_e\| = \frac{2\alpha\omega_m\|\boldsymbol{\omega}_e\|}{k} = 2\alpha\omega_m\|z_2\| \tag{20}$$

Next,

$$\|\frac{J^{-1}}{k}\boldsymbol{\omega}_e^* J\boldsymbol{\omega}_e\| \leq \frac{1}{kJ_m}\sqrt{J_M(J_M - J_m)}\|\boldsymbol{\omega}_e\|^2 = k\sqrt{\alpha(\alpha-1)}\|z_2\|^2 \tag{21}$$

Thus, making use of the bounds calculated in Eq. 20 and 21 and substituting them in Eq. 19 results in

$$\|\frac{J^{-1}\boldsymbol{\Psi}}{k}\| \leq 2\alpha\omega_m\|z_2\| + k\sqrt{\alpha(\alpha-1)}\|z_2\|^2 \tag{22}$$

E. Convergence Analysis

For stability and convergence analysis, consider a Lyapunov-like candidate function

$$\begin{aligned} V = \frac{1}{k}\left[z_1^T z_1 + \frac{3}{2}z_2^T z_2 - z_1^T z_2\right] &= \begin{bmatrix} z_1 & z_2 \end{bmatrix} \underbrace{\frac{1}{k}\begin{bmatrix} \mathbb{I}_{3\times3} & -\frac{1}{2}\mathbb{I}_{3\times3} \\ -\frac{1}{2}\mathbb{I}_{3\times3} & \frac{3}{2}\mathbb{I}_{3\times3} \end{bmatrix}}_{P\in\mathbb{R}^{6\times6}} \begin{bmatrix} z_1 \\ z_2 \end{bmatrix} \\ &= \begin{bmatrix} z_1 & z_2 \end{bmatrix} \left(\underbrace{\frac{1}{k}\begin{bmatrix} 1 & -\frac{1}{2} \\ -\frac{1}{2} & \frac{3}{2} \end{bmatrix}}_{R\in\mathbb{R}^{2\times2}} \otimes \mathbb{I}_{3\times3} \right) \begin{bmatrix} z_1 \\ z_2 \end{bmatrix} \end{aligned} \tag{23}$$

where $\otimes$ denotes the Kronecker product.

We know the maximum and minimum eigenvalues of P and R are equal: $\lambda_{\min}(P) = \lambda_{\min}(R)$

and $\|P\| = \lambda_{\max}(P) = \lambda_{\max}(R)$ which gives us

$$\lambda_{\min}(P) = \frac{5-\sqrt{5}}{4k} = c_1 \tag{24}$$

and

$$\lambda_{\max}(P) = \frac{5+\sqrt{5}}{4k} = c_2 \tag{25}$$

Thus, V defined in Eq. (23) satisfies

$$c_1\|z\|^2 \leq V = z^T P z \leq c_2\|z\|^2 \tag{26}$$

Next, taking the time derivative of V in Eq. (23), followed by substituting Eq. 14 and Eq. 19 results in

$$\begin{aligned}
\dot{V} &= \frac{2}{k} z_1^T \dot{z}_1 + \frac{3}{k} z_2^T \dot{z}_2 - \frac{1}{k} z_1^T \dot{z}_2 - \frac{1}{k} z_2^T \dot{z}_1 \\
&= -z_1^T z_1 - z_2^T z_2 + \frac{3}{k} z_2^T \frac{J^{-1}\boldsymbol{\Psi}}{k} - \frac{1}{k} z_1^T \frac{J^{-1}\boldsymbol{\Psi}}{k} \\
&\leq -\|z\|^2 + \frac{3}{k}\|z_2\| \|\frac{J^{-1}\boldsymbol{\Psi}}{k}\| + \frac{1}{k}\|z_1\| \|\frac{J^{-1}\boldsymbol{\Psi}}{k}\| \\
&\leq -\|z\|^2 + \frac{4}{k}\|z\| \|\frac{J^{-1}\boldsymbol{\Psi}}{k}\|
\end{aligned} \tag{27}$$

Next, using (20) and (21), we have

$$\begin{aligned}
\dot{V} &\leq -\|z\|^2 + \frac{4}{k}\|z\| \left[2\alpha\omega_m\|z\| + k\sqrt{\alpha(\alpha-1)}\|z\|^2\right] \\
&= -\left(1 - \frac{8\alpha\omega_m}{k}\right)\|z\|^2 + 4\sqrt{\alpha(\alpha-1)}\|z\|^3
\end{aligned} \tag{28}$$

To ensure the coefficient of the $\|z\|^2$ term is negative, we select k such that $1 - (8\alpha\omega_m)/k > 0$, i.e.,

$$k > 8\alpha\omega_m \tag{29}$$

Thus, we have

$$\begin{aligned}
\dot{V} &\leq -\left(1 - \frac{8\alpha\omega_m}{k}\right)\|z\|^2 + 4\beta\|z\|^3 \\
\dot{V} &\leq -\|z\|^2 \left[\left(1 - \frac{8\alpha\omega_m}{k}\right) - 4\beta\|z\|\right] \\
&\triangleq -W(z)
\end{aligned} \tag{30}$$

where we introduce the notation $\beta = \sqrt{\alpha(\alpha-1)}$

Define a scalar function $\rho(k)$:

$$\rho(k) \triangleq \frac{1}{4\beta}\left(1 - \frac{8\alpha\omega_m}{k}\right)\sqrt{\frac{c_1}{c_2}} \tag{31}$$

which after substituting the values of c_1 and c_2 respectively from (24) and (25) becomes

$$\rho(k) = \frac{1}{4\beta}\left(1 - \frac{8\alpha\omega_m}{k}\right)\sqrt{\frac{5-\sqrt{5}}{5+\sqrt{5}}} \tag{32}$$

Suppose we restrict initial conditions $z(t_0)$ at time $t_0 = 0$, such that $\|z(t_0)\| \leq \rho(k)$, then using Eq. 30,

$$\begin{aligned} W(z(0)) &= \|z(0)\|^2\left[\left(1 - \frac{8\alpha\omega_m}{k}\right) - 4\beta\|z(0)\|\right] \\ &= 4\beta\|z(0)\|^2\left[\frac{1}{4\beta}\left(1 - \frac{8\alpha\omega_m}{k}\right) - \|z(0)\|\right] \\ &\geq 4\beta\|z(0)\|^2\left[\rho(k)\sqrt{\frac{c_2}{c_1}} - \rho(k)\right] \\ &\geq 0 \end{aligned} \tag{33}$$

since $c_2 > c_1$.

By definition of $W(z)$ in Eq. 30, we know that $\dot{V}(t) \leq 0$ whenever $W(z(t)) \geq 0$. Thus, having a region of attraction $\|z(0)\| \leq \rho(k)$ ensures $\dot{V}(t) \leq 0$ for all $t \geq 0$, that is, $V(t)$ is non-increasing with time. For more details on ROA, the reader is referred to Khalil [17], Chapter 8. Substituting this in (26) leads to

$$c_1\|z(t)\|^2 \leq V(t) \leq V(0) \leq c_2\|z(0)\|^2 \tag{34}$$

Thus,

$$\|z(t)\| \leq \sqrt{\frac{c_2}{c_1}}\|z(0)\| \tag{35}$$

Also, using the definition of $W(z)$ from (30),

$$\begin{aligned} W(z(t)) &= \|z(t)\|^2\left[\left(1 - \frac{8\alpha\omega_m}{k}\right) - 4\beta\|z(t)\|\right] \\ &\geq \|z(t)\|^2\left[\left(1 - \frac{8\alpha\omega_m}{k}\right) - 4\beta\sqrt{\frac{c_2}{c_1}}\|z(0)\|\right] \end{aligned}$$

Defining c_3 to be the terms inside the square brackets,

$$-W(z(t)) \leq -c_3\|z(t)\|^2 \tag{36}$$

Thus we have $\dot{V}(t) \leq -W(z(t)) \leq -c_3\|z(t)\|^2$ or,

$$\begin{aligned} \dot{V}(t) &\leq -\frac{c_3}{c_2}V(t) \\ V(t) &\leq \exp\left(\frac{-c_3 t}{c_2}\right)V(0) \end{aligned} \tag{37}$$

Using this result alongside the inequality from (26) results in

$$\|z(t)\| \leq \sqrt{\frac{c_2}{c_1}} \exp\left(\frac{-c_3 t}{2c_2}\right) \|z(0)\| \tag{38}$$

which proves exponential stability but is a local result for $\|z(0)\| \leq \rho(k)$

F. Discussion

For choosing the value of k, from Eq. 29 we have a lower bound $8\alpha\omega_m$. From (24) and (25) we know, as $k \to \infty$, both $c_1 \to 0$ and $c_2 \to 0$.

However, the ratio

$$\sqrt{\frac{c_1}{c_2}} = \sqrt{\frac{5-\sqrt{5}}{5+\sqrt{5}}} \tag{39}$$

is independent of k. Hence, the upper bound on the initial value of $\|z(0)\|$ given by Eq.31, in the limit becomes

$$\lim_{k\to\infty} \rho(k) = \rho^* = \frac{1}{4\beta}\sqrt{\frac{c_1}{c_2}} = \frac{1}{4\beta}\sqrt{\frac{5-\sqrt{5}}{5+\sqrt{5}}} \tag{40}$$

Thus, the initial condition on the norm of the error states is upper bounded by ρ^* and also lower bounded due to the non-zero positive lower bound on k.

Note that local stability implies specifically, our initial condition $z(0) \in \mathbb{M}$ where

$$\mathbb{M} = \left\{ z \in \mathbb{R}^6 \quad | \quad \|\sigma_e(0)\|^2 + \frac{\|\omega_e(0)\|^2}{k^2} \leq \rho^2(k) \right\} \tag{41}$$

which is the region of attraction. $\sigma_e(0)$ is usually not a restriction because, we can always select $\hat{\sigma}(0) = \sigma(0) \Leftrightarrow \sigma_e(0) = 0$

On the other hand, $\omega_e(0)$ can be arbitrarily large. However, we can always choose large enough k such that irrespective of $\omega_e(t)$,$z(0) \in \mathbb{M}$. In this context, it is crucial that irrespective of how much we increase k, the largest region of attraction ρ^* in Eq. 40 above is a finite constant. Hence, the result is semi-global.

G. Convergence Rate

In (38), $(-c_3/2c_2)$ is the rate of convergence. Note that

$$c_3 = \left(1 - \frac{8\alpha\omega_m}{k}\right) - 4\beta\sqrt{\frac{c_2}{c_1}}\|z(0)\| \tag{42}$$

Thus, as $k \to \infty$, $c_3 \to c_3^*$ where

$$c_3^* = 1 - 4\beta\sqrt{\frac{5+\sqrt{5}}{5-\sqrt{5}}}\|z(0)\| \tag{43}$$

which is independent of k. Also recall that $c_2 \to 0$ as $k \to \infty$. Thus, the rate of convergence $(c_3/2c_2) \to \infty$ as $k \to \infty$. Thus selecting large k implies faster convergence.

III. Adaptive Observer

A. Dynamics and Measurement

Rearranging the dynamics in Eq.1,

$$\begin{aligned}\dot{\boldsymbol{\omega}} &= -J^{-1}\boldsymbol{\omega}^* J\boldsymbol{\omega} + J^{-1}\boldsymbol{\tau} \\ &= \Lambda(\boldsymbol{\omega})\boldsymbol{\theta}^* + W(\boldsymbol{\tau})\boldsymbol{\phi}^*\end{aligned} \tag{44}$$

where $\Lambda : \mathbb{R}^3 \to \mathbb{R}^{3\times 18}$ and $W : \mathbb{R}^3 \to \mathbb{R}^{3\times 6}$ are regressor matrices which are purely functions of the angular rate and torque respectively, $\boldsymbol{\theta}^* \in \mathbb{R}^{18\times 1}$ and $\boldsymbol{\phi}^* \in \mathbb{R}^{6\times 1}$ are vectorized versions of functions of the inertia matrix J terms. The separation of variables to obtain these regressor matrices is detailed in the appendix. Apart from the same assumptions on $\boldsymbol{\omega}$ and $\boldsymbol{\tau}$ as the non-adaptive observer, we additionally assume $\dot{\boldsymbol{\tau}}$ is perfectly determined. The measurements available are the same as the known inertia case, following Eq.2.

B. Objective

The goal is to generate an estimate $\hat{\boldsymbol{\omega}}(t)$ of the true angular rate $\boldsymbol{\omega}(t)$ such that

$$\lim_{t\to\infty} \|\hat{\boldsymbol{\omega}}(t) - \boldsymbol{\omega}(t)\| = 0 \tag{45}$$

without knowledge of the terms of the inertia matrix J and hence without $\boldsymbol{\theta}^*$ and $\boldsymbol{\phi}^*$, keeping all signals bounded.

C. Observer Design

The following observer design is proposed for estimating the angular rate:

$$\dot{\hat{\boldsymbol{\sigma}}} = \hat{\boldsymbol{\omega}} - k(\hat{\boldsymbol{\sigma}} - \boldsymbol{\sigma}) \quad \text{for some } k > 0 \tag{46}$$

$$\dot{\hat{\boldsymbol{\omega}}} = \Lambda(\hat{\boldsymbol{\omega}})(\hat{\boldsymbol{\theta}} + \boldsymbol{\beta}_\theta) + W(\boldsymbol{\tau})(\hat{\boldsymbol{\phi}} + \boldsymbol{\beta}_\phi) - k^2(\hat{\boldsymbol{\sigma}} - \boldsymbol{\sigma}) \tag{47}$$

where $\hat{\boldsymbol{\theta}}$, $\hat{\boldsymbol{\phi}}$, $\boldsymbol{\beta}_\theta$ and $\boldsymbol{\beta}_\phi$ will be defined later. This observer is unique due to the availability of an extra design parameter choice in the form of $\boldsymbol{\beta}_\theta$ and $\boldsymbol{\beta}_\phi$, similar to Immersion and Invariance (I & I) methods [13]. However unlike the I & I method, in this paper, we do not enforce the manifold attractivity condition. As mentioned in the introduction, the linearized transfer function from the measurement $\boldsymbol{\sigma}$ to the unknown parameters $\boldsymbol{\theta}^*$ and $\boldsymbol{\phi}^*$ has two poles at zero, implying that the transfer function is not strictly positive definite, leaving our problem incompatible with the method suggested by Cho and Rajamani [14].

Using the same definition of $z = [z_1, z_2]^T$ from Eq.13, gives us the error dynamics:

$$\dot{z} = k \begin{bmatrix} -\mathbb{I}_{3\times3} & \mathbb{I}_{3\times3} \\ -\mathbb{I}_{3\times3} & \mathbb{O}_{3\times3} \end{bmatrix} z + \frac{1}{k} \begin{bmatrix} \mathbb{O}_{3\times1} \\ \Lambda(\hat{\boldsymbol{\omega}})(\hat{\boldsymbol{\theta}} + \boldsymbol{\beta}_{\boldsymbol{\theta}}) - \Lambda(\boldsymbol{\omega})\boldsymbol{\theta}^* + W(\boldsymbol{\tau})(\hat{\boldsymbol{\phi}} + \boldsymbol{\beta}_{\boldsymbol{\phi}} - \boldsymbol{\phi}^*) \end{bmatrix} \tag{48}$$

The quantity $(\hat{\boldsymbol{\phi}} + \boldsymbol{\beta}_{\boldsymbol{\phi}} - \boldsymbol{\phi}^*)$ takes the physical meaning of the parameter estimation error. Consider the Lyapunov-like candidate function

$$V = \frac{1}{k}\left[z_1^T z_1 + \frac{3}{2} z_2^T z_2 - z_1^T z_2\right] + \frac{1}{2\gamma_1}\|\hat{\boldsymbol{\theta}} + \boldsymbol{\beta}_\theta - \boldsymbol{\theta}^*\|^2 + \frac{1}{2\gamma_2}\|\hat{\boldsymbol{\phi}} + \boldsymbol{\beta}_\phi - \boldsymbol{\phi}^*\|^2 \tag{49}$$

For the inertia terms, let us define error states

$$z_\theta = \hat{\boldsymbol{\theta}} + \boldsymbol{\beta}_\theta - \boldsymbol{\theta}^* \tag{50}$$

$$z_\phi = \hat{\boldsymbol{\phi}} + \boldsymbol{\beta}_\phi - \boldsymbol{\phi}^* \tag{51}$$

and combine these with z to form the full state

$$\boldsymbol{Z} = \begin{bmatrix} z^T & z_\theta^T & z_\phi^T \end{bmatrix}^T \tag{52}$$

Using the constants c_1 and c_2 from Eqs. 24 and 25 respectively, we can bound the function in Eq.49 at any time t as follows:

$$c_1\|z(t)\|^2 \leq V(t) \leq c_2\|z(t)\|^2 + \frac{1}{\gamma_1}\|z_\theta(t)\|^2 + \frac{1}{\gamma_2}\|z_\phi(t)\|^2 \tag{53}$$

The derivative of Eq.49 can be simplified to

$$\begin{aligned} \dot{V} = &-\|z_1\|^2 - \|z_2\|^2 + \frac{1}{k^2}(3z_2 - z_1)^T\left[\Lambda(\hat{\boldsymbol{\omega}}) - \Lambda(\boldsymbol{\omega})\right]\boldsymbol{\theta}^* \\ &+ \frac{1}{k^2}(3z_2 - z_1)^T\left[\Lambda(\hat{\boldsymbol{\omega}})(\hat{\boldsymbol{\theta}} + \boldsymbol{\beta}_\theta - \boldsymbol{\theta}^*) + W(\boldsymbol{\tau})(\hat{\boldsymbol{\phi}} + \boldsymbol{\beta}_\phi - \boldsymbol{\phi}^*)\right] \\ &+ \frac{1}{\gamma_1}(\hat{\boldsymbol{\theta}} + \boldsymbol{\beta}_\theta - \boldsymbol{\theta}^*)^T(\dot{\hat{\boldsymbol{\theta}}} + \dot{\boldsymbol{\beta}}_\theta) + \frac{1}{\gamma_2}(\hat{\boldsymbol{\phi}} + \boldsymbol{\beta}_\phi - \boldsymbol{\phi}^*)^T(\dot{\hat{\boldsymbol{\phi}}} + \dot{\boldsymbol{\beta}}_\phi) \end{aligned} \tag{54}$$

The first three terms of this equation do not involve the inertia estimate error and can follow the same procedure as the non-adaptive case. Thus, if we manage to make the adaptation terms equal zero, we can use the Barbalat's lemma [17] to prove asymptotic convergence to zero of the error states. However, if we did not have the choice of the control knobs $\boldsymbol{\beta}_\theta$ and $\boldsymbol{\beta}_\phi$, the update law $\dot{\hat{\boldsymbol{\theta}}}$ would have to involve $\boldsymbol{z}_2$ which is not an available error state, only $\boldsymbol{z}_1$ is available. This is what necessitates the inclusion of these control knobs we shall now define as:

$$\boldsymbol{\beta}_\theta = \frac{-3\gamma_1}{k^3}\Lambda(\hat{\boldsymbol{\omega}})^T \boldsymbol{z}_1 \tag{55}$$

$$\boldsymbol{\beta}_\phi = \frac{-3\gamma_2}{k^3}W(\boldsymbol{\tau})^T \boldsymbol{z}_1 \tag{56}$$

The derivatives of these terms are:

$$\dot{\boldsymbol{\beta}}_\theta = \frac{3\gamma_1}{k^2}\Lambda(\hat{\boldsymbol{\omega}})^T \boldsymbol{z}_1 - \frac{3\gamma_1}{k^2}\Lambda(\hat{\boldsymbol{\omega}})^T \boldsymbol{z}_2 - \frac{3\gamma_1}{k^3}\left(\frac{\partial \Lambda}{\partial \hat{\omega}}\dot{\hat{\boldsymbol{\omega}}}\right)^T \boldsymbol{z}_1 \tag{57}$$

$$\dot{\boldsymbol{\beta}}_\phi = \frac{3\gamma_2}{k^2}W(\boldsymbol{\tau})^T \boldsymbol{z}_1 - \frac{3\gamma_2}{k^2}W(\boldsymbol{\tau})^T \boldsymbol{z}_2 - \frac{3\gamma_1}{k^3}\left(\frac{\partial W}{\partial \tau}\dot{\boldsymbol{\tau}}\right)^T \boldsymbol{z}_1 \tag{58}$$

Substituting these derivatives back into Eq.54, the $\boldsymbol{z}_2$ term cancels out and for the rest of the inertia error terms, with learning rates γ_1 and γ_2, we choose the following update rules:

$$\dot{\hat{\boldsymbol{\theta}}} = \frac{3\gamma_1}{k^3}\left(\frac{\partial \Lambda}{\partial \hat{\omega}}\dot{\hat{\boldsymbol{\omega}}}\right)^T \boldsymbol{z}_1 - \frac{2\gamma_1}{k^2}\Lambda^T(\hat{\boldsymbol{\omega}})\boldsymbol{z}_1 \tag{59}$$

and

$$\dot{\hat{\boldsymbol{\phi}}} = \frac{3\gamma_2}{k^3}\left(\frac{\partial W}{\partial \tau}\dot{\boldsymbol{\tau}}\right)^T \boldsymbol{z}_1 - \frac{2\gamma_2}{k^2}W^T(\boldsymbol{\tau})\boldsymbol{z}_1 \tag{60}$$

Thus with these choices for the inertia estimate terms, we finally have

$$\dot{V} = -\|\boldsymbol{z}_1\|^2 - \|\boldsymbol{z}_2\|^2 + \frac{1}{k^2}(3\boldsymbol{z}_2 - \boldsymbol{z}_1)^T \left(\Lambda(\hat{\boldsymbol{\omega}}) - \Lambda(\boldsymbol{\omega})\right)\boldsymbol{\theta}^* \tag{61}$$

We know that $\Lambda(\boldsymbol{\omega})\boldsymbol{\theta}^*$ is just a different representation of $J^{-1}\boldsymbol{\omega}^* J\boldsymbol{\omega}$. Thus we can bound the last term in the equation above using Eq. 22:

$$\frac{1}{k}\left(\Lambda(\hat{\boldsymbol{\omega}}) - \Lambda(\boldsymbol{\omega})\right)\boldsymbol{\theta}^* \leq \left(2\alpha\omega_m\|\boldsymbol{z}_2\| + k\beta\|\boldsymbol{z}_2\|^2\right) \tag{62}$$

Going back to Eq. 61,

$$\begin{aligned}
\dot{V} &\leq -\|\boldsymbol{z}\|^2 + \frac{1}{k}\left(3\|\boldsymbol{z}_2\| + \|\boldsymbol{z}_1\|\right)\left(2\alpha\omega_m\|\boldsymbol{z}_2\| + k\beta\|\boldsymbol{z}_2\|^2\right) \\
&\leq -\|\boldsymbol{z}\|^2 + \frac{4}{k}\|\boldsymbol{z}\|^2\left(2\alpha\omega_m + k\beta\|\boldsymbol{z}\|\right) \\
&= -\left(1 - \frac{8\alpha\omega_m}{k}\right)\|\boldsymbol{z}\|^2 + 4\beta\|\boldsymbol{z}\|^3
\end{aligned} \tag{63}$$

where similar to the non-adaptive case, $\alpha = \frac{J_M}{J_m}$ is the ratio of the nominal maximum and minimum

eigenvalues J_M and J_m of J and $\beta = \sqrt{\alpha(\alpha-1)}$. To ensure the first term is negative, we can choose k such that

$$k > 8\omega_m \alpha = 8\omega_m \frac{J_M}{J_m} \tag{64}$$

Since $\boldsymbol{\theta}^*$ is not known in this case, a conservative upper bound on the largest eigenvalue J_M and lower bound on the smallest eigenvalue J_m of the inertia matrix can be used.

Now if we manage to restrict the initial conditions for the states that will make $\dot{V}(t) \leq 0$ for all time $t \geq 0$, we can then have a non-increasing V, that is, $V(t) \leq V(0), \quad \forall t > 0$. If this condition is met, using Eq.53, we have

$$\begin{aligned} c_1\|z(t)\|^2 &\leq c_2\|z(0)\|^2 + \frac{1}{2\gamma_1}\|z_\theta(0)\|^2 + \frac{1}{2\gamma_2}\|z_\phi(0)\|^2 \\ \rightarrow \|z(t)\|^2 &\leq \frac{c_2}{c_1}\|z(0)\|^2 + \frac{1}{2c_1\gamma_1}\|z_\theta(0)\|^2 + \frac{1}{2c_1\gamma_2}\|z_\phi(0)\|^2 \end{aligned} \tag{65}$$

Let us define a new constant

$$\mu_0^2 \triangleq \max\left[\frac{c_2}{c_1}, \frac{1}{2c_1\gamma_1}, \frac{1}{2c_1\gamma_2}\right] \tag{66}$$

which always satisfies $\mu_0 > 1$ since $c_2 > c_1$.

Thus whenever $\dot{V}(t) \leq 0$, we have

$$\begin{aligned} \|z(t)\|^2 &\leq \mu_0^2\left(\|z(0)\|^2 + \|z_\theta(0)\|^2 + \|z_\phi(0)\|^2\right) \\ \rightarrow \|z(t)\| &\leq \mu_0\|\boldsymbol{Z}(0)\| \end{aligned} \tag{67}$$

Since $\|z\| < \|\boldsymbol{Z}\|$, we can modify Eq.63 to

$$\begin{aligned} \dot{V} &\leq -4\beta\|z\|^2\left[\frac{1}{4\mu_0\beta}\left(1 - \frac{8\alpha\omega_m}{k}\right) - \|\boldsymbol{Z}\|\right] \\ &\leq -4\mu_1\beta\|z\|^2 \leq 0 \end{aligned} \tag{68}$$

for an initial region of attraction

$$\|\boldsymbol{Z}(0)\| \leq \frac{1}{4\mu_0\beta}\left(1 - \frac{8\alpha\omega_m}{k}\right) \triangleq \rho_2(k) \tag{69}$$

which differs from Eq.31 by a scaling constant, μ_0 instead of just $\sqrt{\frac{c_2}{c_1}}$, but $\rho_2(k) > 0$ is still positive due to Eq.64, and

$$\mu_1 = \frac{1}{4\mu_0\beta}\left(1 - \frac{8\alpha\omega_m}{k}\right) - \|\boldsymbol{Z}(0)\| > 0 \tag{70}$$

It is to be noted that unlike the non-adaptive case, this upper bound is now on the full state $\boldsymbol{Z}(0)$ and not just on $z(0)$.

Similar to the non-adaptive scenario, if we select $\boldsymbol{Z}(t_0)$ at time $t_0 = 0$ such that $\|\boldsymbol{Z}(0)\| \leq \rho_2(k)$ we can ensure $\dot{V}(t) \leq 0,\ \forall t \geq 0$. Thus, for a small enough initial $\|\boldsymbol{Z}(0)\|$, V is non-increasing and thus $\lim_{t\to\infty} V(t) = V_\infty$ exists. Thus $V \in \mathbb{L}_\infty \to z \in \mathbb{L}_\infty$. Since V is bounded, the terms $\left(\hat{\boldsymbol{\theta}} + \boldsymbol{\beta}_\theta - \boldsymbol{\theta}^*\right)$ and $\left(\hat{\boldsymbol{\phi}} + \boldsymbol{\beta}_\phi - \boldsymbol{\phi}^*\right)$ are also bounded, leaving the derivative of z to also be bounded using Eq. 69, i.e., $\dot{z} \in \mathbb{L}_\infty$. Integrating Eq.68 on both sides,

$$\begin{aligned}
\int_0^\infty \dot{V} dt &\leq \int_0^\infty -4\beta\mu_1 \|z\|^2 dt \\
V_\infty - V(0) &\leq -4\beta\mu_1 \int_0^\infty \|z\|^2 dt \\
\int_0^\infty \|z\|^2 dt &\leq \frac{V(0) - V_\infty}{4\beta\mu_1}
\end{aligned} \tag{71}$$

which implies $z \in \mathbb{L}_2$. Thus using the corollary to the Barbalat's lemma, since $z \in \mathbb{L}_2 \cap \mathbb{L}_\infty$ and $\dot{z} \in \mathbb{L}_\infty$, we have $\lim_{t\to\infty} z(t) = 0$. Thus the observer errors in attitude and angular rate asymptotically converge to zero. The errors in the estimates of the inertia terms z_θ and z_ϕ will also converge to zero subject to adequate persistence of excitation.

D. Discussion

Similar to the non-adaptive case, the user chosen parameter k and the trajectory followed by the system impact the region of attraction for $\|\boldsymbol{Z}(0)\|$ within which all initial values of error state $\|z\|$ will asymptotically converge to zero with adaptation for the inertia terms. It is important to note that Eq.69 is different from the non-adaptive case since it is the region of attraction for the norm of the full state including the inertia error terms. If we know an upper bound on the error in the initial guess of $\boldsymbol{\theta}^*$ and $\boldsymbol{\phi}^*$, that is $\|z_\theta(0)\| < \|\tilde{\boldsymbol{\theta}}\|$ and $\|z_\phi(0)\| < \|\tilde{\boldsymbol{\phi}}\|$, we can then state that the observer estimate of the attitude and rate will converge to the true values if

$$\|z(0)\| \leq \rho_2(k) - \|\tilde{\boldsymbol{\theta}}\| - \|\tilde{\boldsymbol{\phi}}\| \tag{72}$$

This is clearly smaller than the region of attraction for $\|z(0)\|$ in the non-adaptive scenario by the magnitude of $\|\tilde{\boldsymbol{\theta}}\| + \|\tilde{\boldsymbol{\phi}}\|$, which is the price to pay for adaptation, along with sacrificing exponential convergence for asymptotic convergence.

While the size of α affects our choice of k, the upper bound on $\|\boldsymbol{Z}(0)\|$ in Eq.69 in the limit is

still non-zero, as in the non-adaptive scenario:

$$\lim_{k\to\infty} \rho_2(k) = \frac{1}{4\beta\mu_0} \tag{73}$$

This indicates that the result is once again semi-global since irrespective of the choice of k, $1/4\beta$ is the lower bound on the region of attraction for the full initial state $\|\boldsymbol{Z}(0)\|$. However, this demonstrates how being overly conservative and choosing large values of α (since $\beta = \sqrt{\alpha(\alpha-1)}$) makes our region of attraction smaller for the initial state. On the other hand if α is chosen smaller than the true value, the choice of k from Eq. 64 could in turn be too small and impact the convergence properties of the observer to the true state.

The discussion from the non-adaptive section holds, that we have the option to choose the attitude error state $\boldsymbol{\sigma_e}(0)$ to be zero initially by selecting $\hat{\boldsymbol{\sigma}}(0) = \boldsymbol{\sigma}(0)$ but $\boldsymbol{\omega}_e(0)$ can be arbitrarily large. Selecting k large enough can accommodate this since higher k still leads to a larger $\rho_2(k)$. However, higher values of k should also be accompanied by higher values of γ_1 and γ_2 since the adaptation Eqs. 57 - 60 become sluggish with higher k.

The estimates $\hat{\boldsymbol{\theta}} + \boldsymbol{\beta_\theta}$ and $\hat{\boldsymbol{\phi}} + \boldsymbol{\beta_\phi}$ converge to the true values of $\boldsymbol{\theta}^*$ and $\boldsymbol{\phi}^*$ when we have an applied torque that is rich enough or persistently exciting (PE). It is important to note that we still require the angular velocity to be bounded. Moreover, while a PE torque helps with the estimation of the inertia parameters, it is not required for the RIG observer estimates of the attitude and angular velocity to converge to their true values, which is guaranteed for any known and bounded torque with initial states satisfying Eq. 69.

A special case to be noted is when there is no torque acting on the system. If $\boldsymbol{\tau}$ is identically zero, we can avoid adapting for $\boldsymbol{\phi}$ since $W(\boldsymbol{\tau}) = 0$ in Eq.47 and thus leave out the $\boldsymbol{z}_\phi$ term from the Lyapunov function in Eq.49. This also implies that $\tilde{\phi} = 0$ and we can have a bigger region of attraction for the attitude and rate states in Eq.72 using the same Lyapunov analysis as above without any of the terms involving $\boldsymbol{z}_\phi$ and the ROA for the full state, $\rho_2(k)$ does not change:

$$\|\boldsymbol{z}(0)\| \leq \rho_2(k) - \|\tilde{\boldsymbol{\theta}}\| \tag{74}$$

IV. Robustness Analysis

There can be scenarios when the adaptive observer cannot be used due to it's increased complexity or just not required for minor inaccuracies in inertia. For such cases, we consider the robustness properties of the non-adaptive observer from Eqs. 4 and 5 in two different scenarios:

- The external torque $\boldsymbol{\tau}$ is unavailable but is bounded and an upper bound is known $\boldsymbol{\tau} \in \mathbb{L}_\infty$, i.e., there exists some finite $\tau_m = \sup_{t\geq 0} \|\boldsymbol{\tau}(t)\|$. Can the observer be ensured to converge to a residual set?
- The inertia matrix J is inaccurately modelled as $\bar{J} = \bar{J}^T > 0$ (nominal inertia) and thus, there is an inertia error $(J - \bar{J})$? Can the observer errors be bounded in this setting?

We provide positive answers to both these cases in the sequel.

A. Unknown Torque

We assume some bounded unknown external torque $\boldsymbol{\tau}$ acting upon the spacecraft. The non-adaptive observer is modified to:

$$\dot{\hat{\boldsymbol{\sigma}}} = \hat{\boldsymbol{\omega}} - k(\hat{\boldsymbol{\sigma}} - \boldsymbol{\sigma}) \tag{75}$$

$$J\dot{\hat{\boldsymbol{\omega}}} = -\hat{\boldsymbol{\omega}}^* J\hat{\boldsymbol{\omega}} - k^2 J(\hat{\boldsymbol{\sigma}} - \boldsymbol{\sigma}) \tag{76}$$

This leads to

$$\dot{\boldsymbol{\sigma}}_e = -k\boldsymbol{\sigma}_e + k\left(\frac{\boldsymbol{\omega}_e}{k}\right) \tag{77}$$

$$\frac{\dot{\boldsymbol{\omega}}_e}{k} = -k\boldsymbol{\sigma}_e + \frac{J^{-1}}{k}\boldsymbol{\Psi} - \frac{J^{-1}}{k}\boldsymbol{\tau} \tag{78}$$

$$\Leftrightarrow \dot{\boldsymbol{z}} = k\begin{bmatrix} -\mathbb{I} & \mathbb{I} \\ -\mathbb{I} & 0 \end{bmatrix}\boldsymbol{z} + \begin{bmatrix} 0 \\ \frac{J^{-1}}{k}\boldsymbol{\Psi} \end{bmatrix} + \begin{bmatrix} 0 \\ -\frac{J^{-1}}{k}\boldsymbol{\tau} \end{bmatrix} \tag{79}$$

where the last term is defined as the disturbance

$$\boldsymbol{d} \triangleq \begin{bmatrix} 0 \\ -\frac{J^{-1}}{k}\boldsymbol{\tau} \end{bmatrix} \tag{80}$$

For the case with known torque ($\boldsymbol{d} = 0$), we already have from Eq. 36, a Lyapunov function such

that

$$c_1\|z\|^2 \leq V(z) \leq c_2\|z\|^2 \tag{81}$$

$$\dot{V} \triangleq \left(\frac{\partial V}{\partial z}\right)^T \dot{z} \leq -c_3\|z\|^2 \tag{82}$$

Also recall

$$V(z) = \frac{1}{k}\left(z_1^T z_1 + \frac{3}{2}z_2^T z_2 - z_1^T z_2\right) = z^T P z \tag{83}$$

Thus, $\frac{\partial V}{\partial z} = 2Pz$

$$\Leftrightarrow \|\frac{\partial V}{\partial z}\| \leq 2\lambda_{\max}(P)\|z\| = 2c_2\|z\| \tag{84}$$

since $\|P\| = \lambda_{\max}(P) = c_2 = (5+\sqrt{5})/4k$.

If we define $c_4 = 2c_2$, the above equation can be written as $\|\frac{\partial V}{\partial z}\| \leq c_4\|z\|$. Next recall,

$$\boldsymbol{d} = \begin{bmatrix} 0 \\ -\frac{J^{-1}}{k}\boldsymbol{\tau} \end{bmatrix} \Leftrightarrow \|\boldsymbol{d}\| \leq \frac{\tau_m}{kJ_m} \tag{85}$$

Suppose for some $\theta \in (0,1)$,

$$\frac{\tau_m}{kJ_m} < \frac{c_3}{c_4}\sqrt{\frac{c_1}{c_2}}\theta\rho(k) \tag{86}$$

this implies that there exists k sufficiently large such that

$$\tau_m < \frac{c_3}{c_4}\sqrt{\frac{c_1}{c_2}}\theta k J_m \rho(k) \tag{87}$$

Then using Lemma 9.2 from Khalil [17], for all $\|z(0)\| < \sqrt{c_1/c_2}\rho(k)$, we have

$$\|z(t)\| \leq \sqrt{\frac{c_2}{c_1}}\exp\left(-\gamma(t)\right)\|z(0)\| \quad \forall\ 0 \leq t \leq T \tag{88}$$

and

$$\|z(t)\| \leq b \text{ for } t \geq T \tag{89}$$

which is a residual set and a uniform ultimate bound for some finite $T > 0$, where

$$\gamma = \frac{(1-\theta)c_3}{2c_2} \tag{90}$$

and

$$b = \frac{c_4}{c_3}\sqrt{\frac{c_2}{c_1}}\frac{\tau_m}{J_m k\theta} \tag{91}$$

note that $b \to 0$ as $k \to \infty$.

B. Inaccurate Inertia Model

If the inertia matrix J is poorly modeled, a nominal inertia $\bar{\boldsymbol{J}}$ is adopted with maximum and minimum eigenvalues $\bar{J}_M$ and $\bar{J}_m$ respectively. We modify the observer to be:

$$\dot{\hat{\boldsymbol{\sigma}}} = \hat{\boldsymbol{\omega}} - k(\hat{\boldsymbol{\sigma}} - \boldsymbol{\sigma}) \tag{92}$$

$$\dot{\hat{\boldsymbol{\omega}}} = -k^2(\hat{\boldsymbol{\sigma}} - \boldsymbol{\sigma}) - \bar{J}^{-1}\hat{\boldsymbol{\omega}}^* \bar{J}\hat{\boldsymbol{\omega}} + \bar{J}^{-1}\boldsymbol{\tau} \tag{93}$$

such that the disturbance term in Eq. 80 can be modified as follows

$$\bar{\boldsymbol{d}} = \begin{bmatrix} 0 \\ -\frac{1}{k}(\bar{J}^{-1}\boldsymbol{\omega}^* \bar{J}\boldsymbol{\omega} - J^{-1}\boldsymbol{\omega}^* J\boldsymbol{\omega}) + (\bar{J}^{-1} - J^{-1})\boldsymbol{\tau}) \end{bmatrix} \tag{94}$$

The nominal system, i.e., with $\bar{\boldsymbol{d}} = 0$, provides us with the same behavior as the unknown torque case above, hence (88) and (89) hold with the convergence rate in (90). However, the modified ratio of eigenvalues of the inertia matrix, α is replaced by $\bar{\alpha} = \bar{J}_M/\bar{J}_m$ and the residual set to which the norm of the states converges to is now:

$$b = \frac{c_4}{c_3}\sqrt{\frac{c_2}{c_1}}\frac{1}{J_m \bar{J}_m k\theta}\left[\tau_m(\bar{J}_m + J_m) + \omega_m^2(J_M \bar{J}_m + \bar{J}_M J_m)\right] \tag{95}$$

This proves that the proposed observer is robust to inaccuracies in the inertia matrix and unknown external torques, with the angular velocity estimates always converging to a local residual region surrounding the true value of the state.

V. Simulations

We perform numerical simulations for a spacecraft with an inertia matrix:

$$J = \begin{bmatrix} 20 & 1.2 & 0.9 \\ 1.2 & 17 & 1.4 \\ 0.9 & 1.4 & 15 \end{bmatrix} \tag{96}$$

starting from $\boldsymbol{\omega}(\mathbf{0}) = [0.1, 0.05, 0]^T$.

The external torques are chosen as

$$\boldsymbol{\tau_1} = \begin{bmatrix} 0.1\sin(t) \\ 0.2\cos(2t) \\ 0.3\cos(3t) \end{bmatrix} \tag{97}$$

and a persistently exciting

$$\boldsymbol{\tau_2} = \begin{bmatrix} 0.1\cos(2t) + 0.2 \\ 0.5\cos(2t) + 0.4 \\ 0.1\sin(2t) + 0.2 \end{bmatrix} \tag{98}$$

For the case when the inertia and torque are known accurately, the error in velocity is shown in Fig. 1 for J, $\boldsymbol{\tau_1}$ and $k = 20$, where the estimate can be clearly seen to be converging to the real values of the angular velocity and the errors go to zero.

For demonstrating the robustness properties of the observer, we use the system with inertia J from Eq.96 with the non-adaptive observer using an inertia estimate of

$$\bar{J} = \begin{bmatrix} 21 & 2.2 & 1.9 \\ 2.2 & 18 & 2.4 \\ 1.9 & 2.4 & 16 \end{bmatrix} \tag{99}$$

which represents approximately 5% error in the inertia parameter model. The torque input from Eq. 97 was applied to the system but is unknown to the observer. The angular velocity and norm of the error states are shown in Fig. 2, where once again, the estimate converges to the true state, demonstrating the robustness of the observer to inertia and torque inaccuracies.

To demonstrate the working of the adaptive observer, we use the same inertia matrix J above. Fig.3a shows the norm of the angular velocity error for an initial inertia guess of $\bar{J}$ above acted upon by τ_1, while Fig.3b shows the same results for an initial inertia error of 20% of J with τ_2. Fig.4 compares the norm of the full error state for the non-adaptive and adaptive observers. If we consider the parameter estimation error to be represented by

$$\tilde{\phi} = \|\hat{\boldsymbol{\phi}} + \boldsymbol{\beta_\phi} - \boldsymbol{\phi}^*\| \tag{100}$$

Fig. 5 shows $\tilde{\phi}$ for J with a persistently exciting torque $\boldsymbol{\tau_2}$, which clearly goes down to zero,

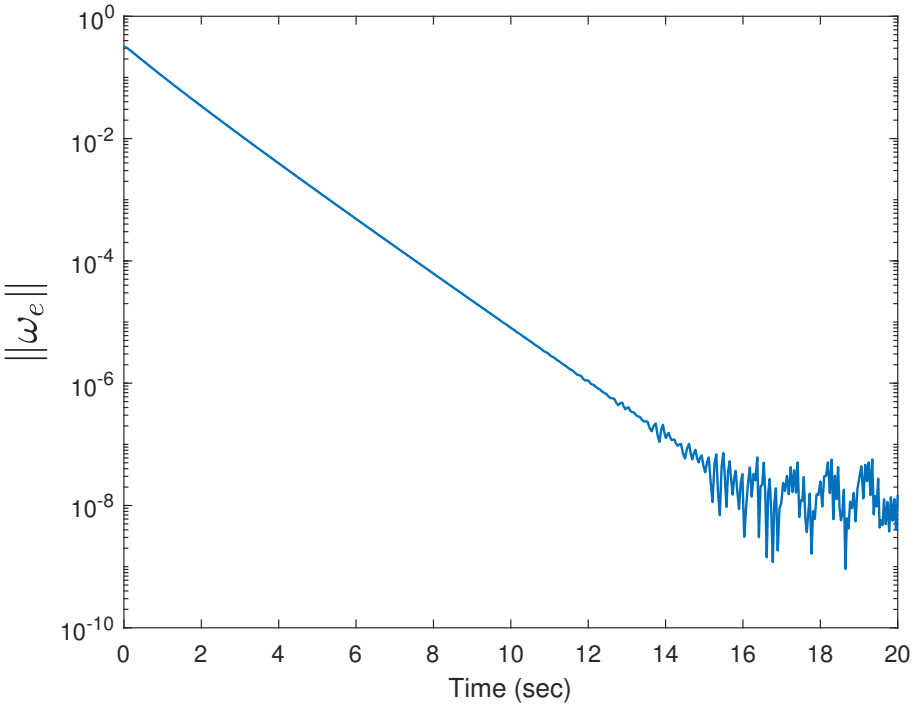

Fig. 1 Angular velocity estimation error for non-adaptive known torque and inertia

demonstrating the convergence of the estimate to the true values of the terms of the inertia matrix. The inertia matrix can be retrieved from the estimate $\hat{\boldsymbol{\phi}}$ if required.

VI. Conclusions

A novel observer was designed for estimating the full attitude and angular rate states from the continuous measurements of a Rate Integrating Gyroscope (RIG), along with an adaptation modification for when the inertia of the system is not accurately characterized. The observer was shown using a Lyapunov-like analysis to drive the angular velocity estimates to their true values exponentially fast when the inertia is known and asymptotically converge in the adaptive case. The update laws are linear in the measurement term and involve one user chosen parameter which controls the convergence rate of the estimate and the region of attraction for the initial value of the state. The non-adaptive observer was also shown to be robust to an inaccurately modeled inertia matrix as well as unknown torque inputs to the system. The effectiveness of the design was proven numerically in simulations.

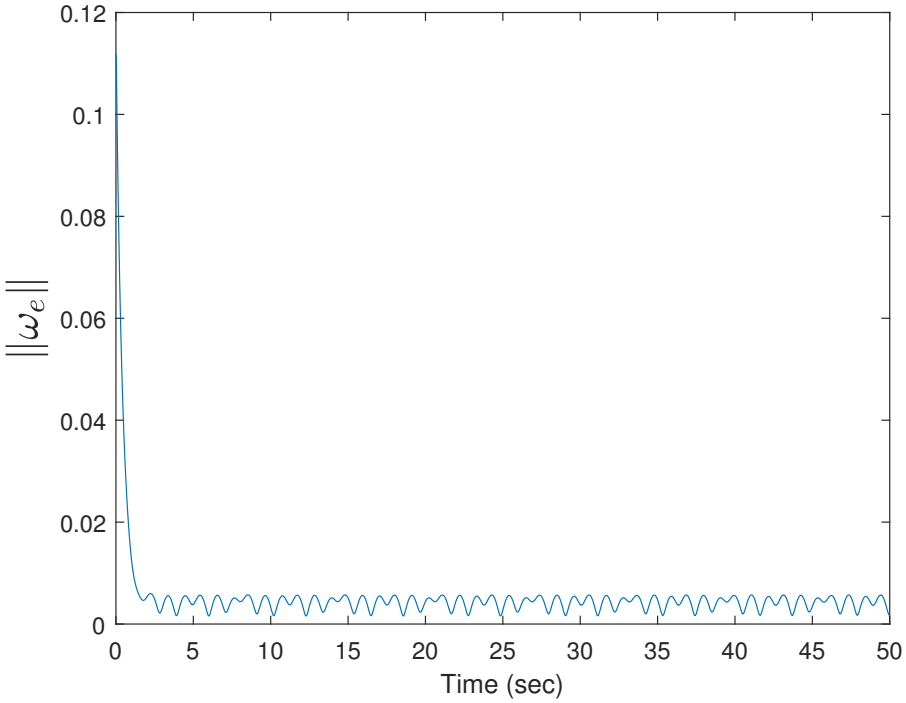

(a) Angular velocity estimation error for $\bar{J}$

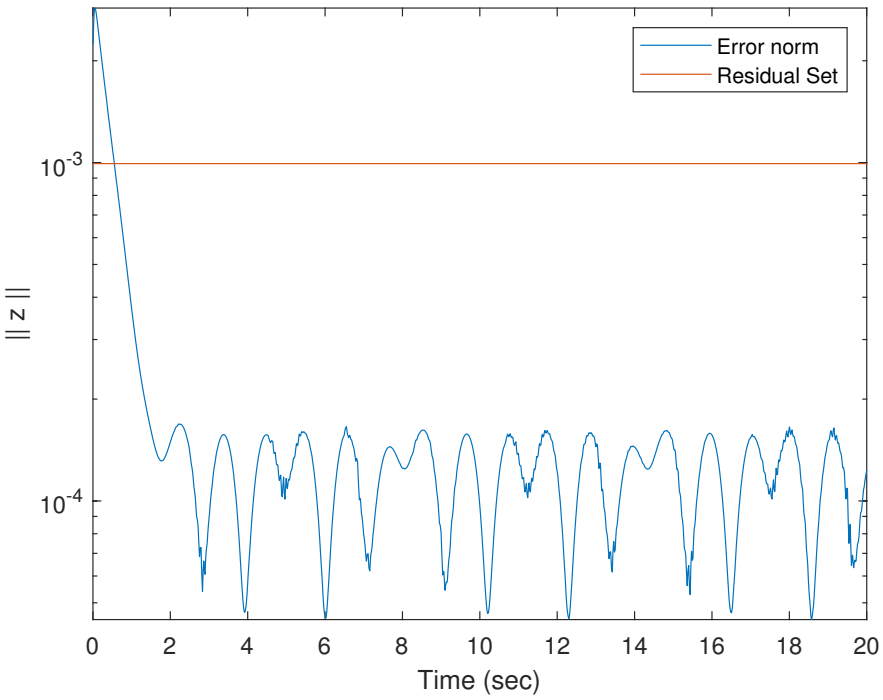

(b) Norm of full error state

Fig. 2 Simulations for the non-adaptive inaccurate inertia and unknown torque case

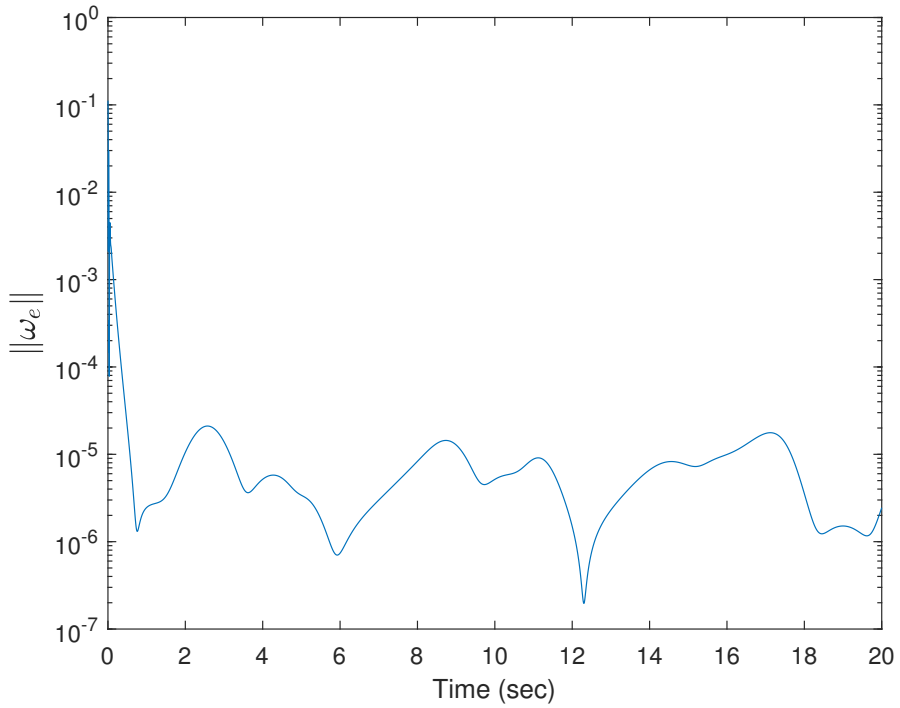

(a) Adaptive angular velocity estimation error norm for J_1

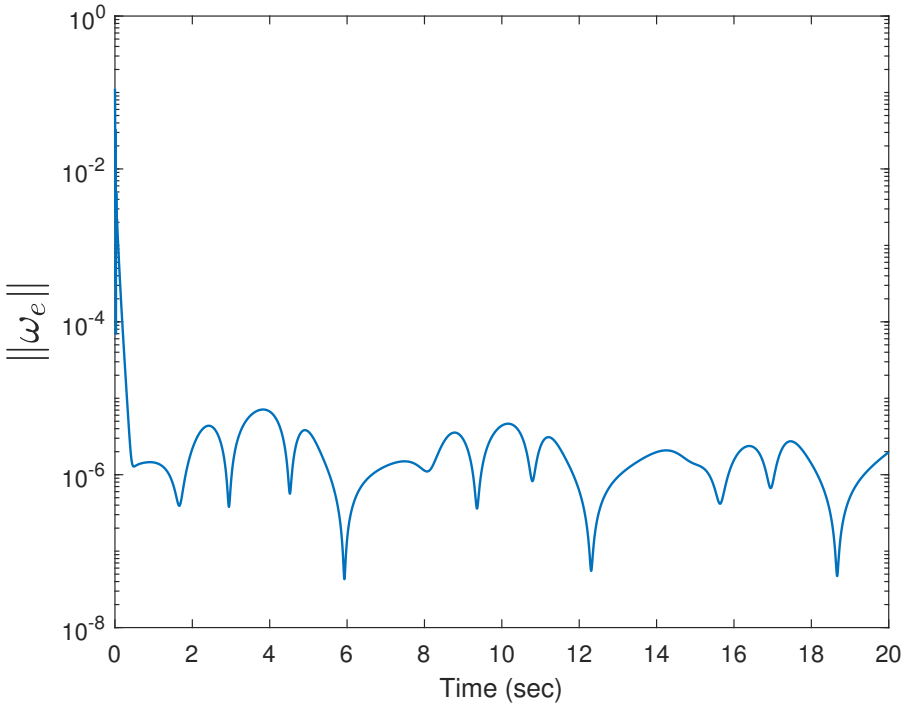

(b) Adaptive angular velocity estimation error norm for Cassini J_2 [18]

Fig. 3 Simulations for adaptive inertia and known torque

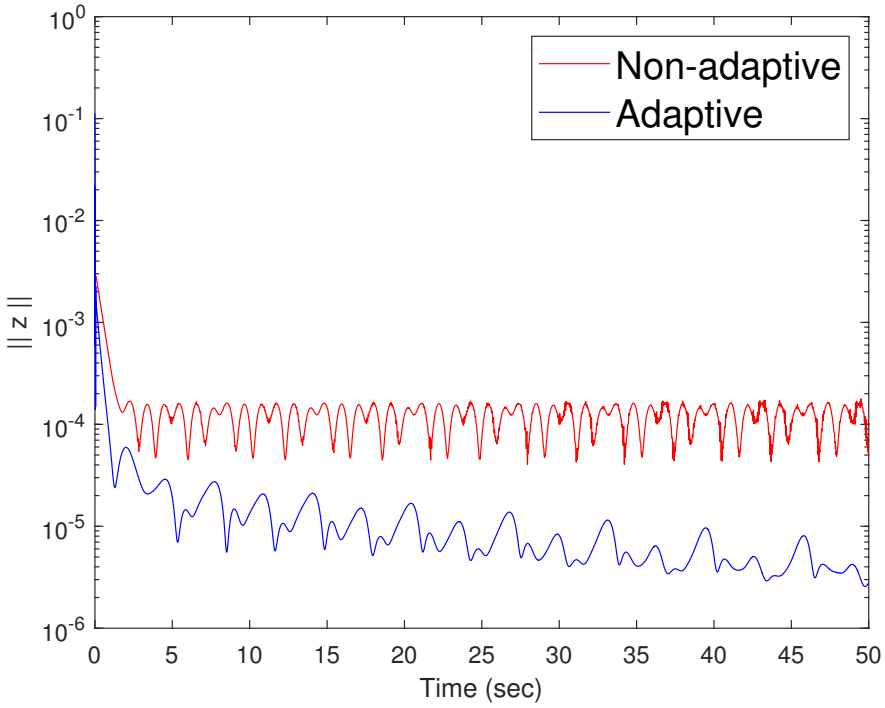

Fig. 4 Comparison of the norm of full error states - Adaptive vs non adaptive

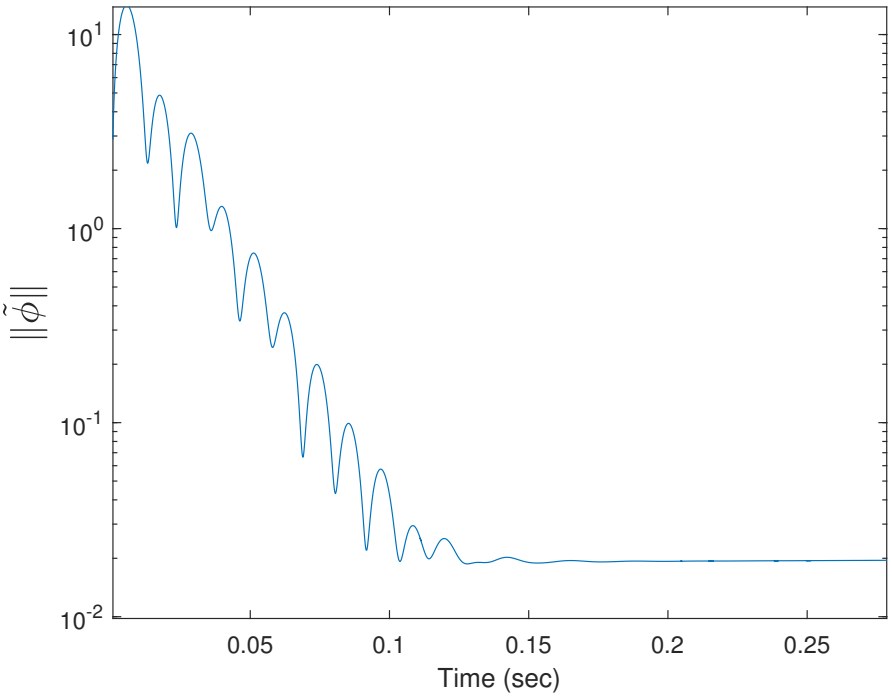

Fig. 5 Norm of the parameter estimation error for ϕ

References

[1] Savage, P. G., "Strapdown inertial navigation integration algorithm design part 2: Velocity and position algorithms," *Journal of Guidance, Control, and Dynamics*, Vol. 21, No. 2, 1998, pp. 208–221.

[2] Crassidis, J. L., Markley, F. L., and Cheng, Y., "Survey of Nonlinear Attitude Estimation Methods," *Journal of Guidance, Control, and Dynamics*, Vol. 30, No. 1, 2007, pp. 12–28. doi:10.2514/1.22452, URL https://doi.org/10.2514/1.22452.

[3] Kinsey, J. C., Eustice, R. M., and Whitcomb, L. L., "A survey of underwater vehicle navigation: Recent advances and new challenges," *IFAC Conference of Manoeuvering and Control of Marine Craft*, Vol. 88, Lisbon, 2006, pp. 1–12.

[4] Fallah, N., Apostolopoulos, I., Bekris, K., and Folmer, E., "Indoor human navigation systems: A survey," *Interacting with Computers*, Vol. 25, No. 1, 2013, pp. 21–33.

[5] Barshan, B., and Durrant-Whyte, H. F., "Inertial navigation systems for mobile robots," *IEEE transactions on robotics and automation*, Vol. 11, No. 3, 1995, pp. 328–342.

[6] Markley, F. L., and Crassidis, J. L., *Fundamentals of spacecraft attitude determination and control*, Vol. 33, Springer, 2014.

[7] Senkal, D., Ng, E., Hong, V., Yang, Y., Ahn, C., Kenny, T., and Shkel, A., "Parametric drive of a toroidal MEMS rate integrating gyroscope demonstrating< 20 PPM scale factor stability," *2015 28th IEEE International Conference on Micro Electro Mechanical Systems (MEMS)*, IEEE, 2015, pp. 29–32.

[8] Pai, P., Pourzand, H., and Tabib-Azar, M., "Magnetically coupled resonators for rate integrating gyroscopes," *SENSORS, 2014 IEEE*, IEEE, 2014, pp. 1173–1176.

[9] Crassidis, J. L., and Markley, F. L., "Three-axis attitude estimation using rate-integrating gyroscopes," *Journal of Guidance, Control, and Dynamics*, Vol. 39, No. 7, 2016, pp. 1513–1526.

[10] Friedkand, B., "Estimating Angular Velocity from Output of Rate-integrating Gyro," *IEEE Transactions on Aerospace and Electronic Systems*, Vol. AES-11, No. 4, 1975, pp. 551–555. doi:10.1109/TAES.1975.308119.

[11] Grip, H. F., Fossen, T. I., Johansen, T. A., and Saberi, A., "Globally exponentially stable attitude and gyro bias estimation with application to GNSS/INS integration," *Automatica*, Vol. 51, 2015, pp. 158 – 166.

[12] Berkane, S., Abdessameud, A., and Tayebi, A., "A globally exponentially stable hybrid attitude and gyro-bias observer," *2016 IEEE 55th Conference on Decision and Control (CDC)*, 2016, pp. 308–313.

[13] Astolfi, A., and Ortega, R., "Immersion and invariance: a new tool for stabilization and adaptive control of nonlinear systems," *IEEE Transactions on Automatic Control*, Vol. 48, No. 4, 2003, pp. 590–606. doi:10.1109/TAC.2003.809820.

[14] Cho, Y. M., and Rajamani, R., "A systematic approach to adaptive observer synthesis for nonlinear systems," *IEEE transactions on Automatic Control*, Vol. 42, No. 4, 1997, pp. 534–537.

[15] Marino, R., and Tomei, P., "Adaptive observers with arbitrary exponential rate of convergence for nonlinear systems," *IEEE Transactions on Automatic Control*, Vol. 40, No. 7, 1995, pp. 1300–1304.

[16] Besançon, G., "Remarks on nonlinear adaptive observer design," *Systems & control letters*, Vol. 41, No. 4, 2000, pp. 271–280.

[17] Khalil, H. K., *Nonlinear systems*, Vol. 3, Prentice hall Upper Saddle River, NJ, 2002.

[18] Lee, A. Y., and Wertz, J. A., "In-Flight Estimation of the Cassini Spacecraft's Inertia Tensor," *Journal of Spacecraft and Rockets*, Vol. 39, No. 1, 2002, pp. 153–155. doi:10.2514/2.3795, URL `https://doi.org/10.2514/2.3795`.

Appendices

A. Regressor Matrix θ^*

Consider the dynamics from Eq.1 rearranged as Eq.44.

$$\dot{\boldsymbol{\omega}} = -J^{-1}\boldsymbol{\omega}^* J\boldsymbol{\omega} + J^{-1}\boldsymbol{\tau} \tag{101}$$

Let the symmetric inertia matrix have components

$$J = \begin{bmatrix} J_{11} & J_{12} & J_{13} \\ J_{12} & J_{22} & J_{23} \\ J_{13} & J_{23} & J_{33} \end{bmatrix} \tag{102}$$

Using the eigenvectors v_1, v_2 and v_3 of J, there exists an orthogonal matrix R:

$$R = \begin{bmatrix} \uparrow & \uparrow & \uparrow \\ v_1 & v_2 & v_3 \\ \downarrow & \downarrow & \downarrow \end{bmatrix} \tag{103}$$

which converts the inertia to the principal axis frame as matrix D which has all its off-diagonal terms to be zero such that:

$$J = RDR^T \tag{104}$$

and

$$J^{-1} = RD^{-1}R^T \tag{105}$$

where $D = \text{diag}[D_1, D_2, D_3]$, and $R^T R = I_{3\times 3}$. However, since J is now known, we do not know the matrices D or R, which are functions of the terms of the inertia matrix.

Now consider the term $J^{-1}\boldsymbol{\omega}^* J\boldsymbol{\omega}$. Substituting for the value of J,

$$\begin{aligned} J^{-1}\boldsymbol{\omega}^* J\boldsymbol{\omega} &= RD^{-1}R^T\boldsymbol{\omega}^* RDR^T\boldsymbol{\omega} \\ &= RD^{-1}\left(R^T\boldsymbol{\omega}\right)^* R^T RDR^T\boldsymbol{\omega} \\ &= RD^{-1}\boldsymbol{\eta}^* D\boldsymbol{\eta} \end{aligned} \tag{106}$$

where $\boldsymbol{\eta} = [\eta_1, \eta_2, \eta_3]^T = R^T\boldsymbol{\omega}$.

Since D is a diagonal matrix, we also have

$$\boldsymbol{\eta}^* D\boldsymbol{\eta} = \begin{bmatrix} D_2 - D_3 & 0 & 0 \\ 0 & D_3 - D_1 & 0 \\ 0 & 0 & D_1 - D_2 \end{bmatrix} \begin{bmatrix} \eta_2\eta_3 \\ \eta_3\eta_1 \\ \eta_1\eta_2 \end{bmatrix} = S \begin{bmatrix} \eta_2\eta_3 \\ \eta_3\eta_1 \\ \eta_1\eta_2 \end{bmatrix} \tag{107}$$

Using the vector Kronecker product,

$$\boldsymbol{\eta} \otimes \boldsymbol{\eta} = \left[\eta_1^2, \eta_1\eta_2, \eta_1\eta_3, \eta_2\eta_1, \eta_2^2, \eta_2\eta_3, \eta_3\eta_1, \eta_3\eta_2, \eta_3^2\right]^T \tag{108}$$

we have

$$\begin{bmatrix} \eta_2\eta_3 \\ \eta_3\eta_1 \\ \eta_1\eta_2 \end{bmatrix} = \begin{bmatrix} 0 & 0 & 0 & 0 & 0 & 1 & 0 & 0 & 0 \\ 0 & 0 & 1 & 0 & 0 & 0 & 0 & 0 & 0 \\ 0 & 1 & 0 & 0 & 0 & 0 & 0 & 0 & 0 \end{bmatrix} \boldsymbol{\eta} \otimes \boldsymbol{\eta} = M(\boldsymbol{\eta} \otimes \boldsymbol{\eta}) \tag{109}$$

Also

$$\boldsymbol{\eta} \otimes \boldsymbol{\eta} = R^T\boldsymbol{\omega} \otimes R^T\boldsymbol{\omega} = (R^T \otimes R^T)(\boldsymbol{\omega} \otimes \boldsymbol{\omega}) \tag{110}$$

Thus

$$J^{-1}\boldsymbol{\omega}^* J\boldsymbol{\omega} = RD^{-1}SM(R^T \otimes R^T)(\boldsymbol{\omega} \otimes \boldsymbol{\omega}) \tag{111}$$

Since $\boldsymbol{\omega} \otimes \boldsymbol{\omega}$ has duplicate entries, we can reduce redundancies by using

$$\boldsymbol{\omega} \otimes \boldsymbol{\omega} = \begin{bmatrix} \omega_1^2 \\ \omega_1\omega_2 \\ \omega_1\omega_3 \\ \omega_2\omega_1 \\ \omega_2^2 \\ \omega_2\omega_3 \\ \omega_3\omega_1 \\ \omega_3\omega_2 \\ \omega_3^2 \end{bmatrix} = \begin{bmatrix} 1 & 0 & 0 & 0 & 0 & 0 \\ 0 & 1 & 0 & 0 & 0 & 0 \\ 0 & 0 & 1 & 0 & 0 & 0 \\ 0 & 1 & 0 & 0 & 0 & 0 \\ 0 & 0 & 0 & 1 & 0 & 0 \\ 0 & 0 & 0 & 0 & 1 & 0 \\ 0 & 0 & 1 & 0 & 0 & 0 \\ 0 & 0 & 0 & 0 & 1 & 0 \\ 0 & 0 & 0 & 0 & 0 & 1 \end{bmatrix} \begin{bmatrix} \omega_1^2 \\ \omega_1\omega_2 \\ \omega_1\omega_3 \\ \omega_2^2 \\ \omega_2\omega_3 \\ \omega_3^2 \end{bmatrix} \triangleq N\boldsymbol{\Omega} \tag{112}$$

Hence

$$\begin{aligned} J^{-1}\boldsymbol{\omega}^* J\boldsymbol{\omega} &= RD^{-1}SM(R^T \otimes R^T)N\boldsymbol{\Omega} \\ &= \Lambda(\boldsymbol{\omega})\mathrm{vec}\left(RD^{-1}SM(R^T \otimes R^T)N\right) \\ &= \Lambda(\boldsymbol{\omega})\boldsymbol{\theta}^* \end{aligned} \tag{113}$$

where vec is the vectorization operation along the row and using $\mathbf{\Omega}$ from Eq.112,

$$\Lambda(\omega) = \begin{bmatrix} \mathbf{\Omega}^T & 0 & 0 \\ 0 & \mathbf{\Omega}^T & 0 \\ 0 & 0 & \mathbf{\Omega}^T \end{bmatrix} \tag{114}$$

and

$$\boldsymbol{\theta}^* = \text{vec}\left(RD^{-1}SM(R^T \otimes R^T)N\right) \tag{115}$$

Thus we have managed to separate the components of $\boldsymbol{\omega}$ from the cross product term and consolidated all the unknown inertia component into one vector which can be estimated using the adaptive control method proposed in this paper.

B. Regressor Matrix $\boldsymbol{\phi}^*$

Similar to the previous section, consider next the term $J^{-1}\boldsymbol{\tau}$. By performing symbolic multiplication and then partial differentiation with respect to the torque terms, we have

$$J^{-1}\boldsymbol{\tau} = \begin{bmatrix} \tau_1 & 0 & 0 & \tau_2 & -\tau_3 & 0 \\ 0 & \tau_2 & 0 & \tau_1 & 0 & \tau_3 \\ 0 & 0 & \tau_3 & 0 & -\tau_1 & \tau_2 \end{bmatrix} \begin{bmatrix} J_{22}J_{33} - J_{23}^2 \\ J_{11}J_{33} - J_{13}^2 \\ J_{11}J_{22} - J_{12}^2 \\ J_{13}J_{23} - J_{12}J_{33} \\ J_{22}J_{13} - J_{12}J_{23} \\ J_{12}J_{13} - J_{11}J_{23} \end{bmatrix} / \det(J) = W(\boldsymbol{\tau})\boldsymbol{\phi}^* \tag{116}$$

where det is the determinant of the matrix and $\boldsymbol{\phi}^*$ has all the inertia terms.